Article

TRANSPARENT PROCESS

THE EMBO JOURNAL

Postmitotic diversification of olfactory neuron types is mediated by differential activities of the HMG-box transcription factor SOX-2

Amel Alqadah[1,2,†], Yi-Wen Hsieh[1,†], Berta Vidal[3], Chieh Chang[1], Oliver Hobert[3,‡,**] & Chiou-Fen Chuang[1,‡,*]

Abstract

Diversification of neuron classes is essential for functions of the olfactory system, but the underlying mechanisms that generate individual olfactory neuron types are only beginning to be understood. Here we describe a role of the highly conserved HMG-box transcription factor SOX-2 in postmitotic specification and alternative differentiation of the *Caenorhabditis elegans* AWC and AWB olfactory neurons. We show that SOX-2 partners with different transcription factors to diversify postmitotic olfactory cell types. SOX-2 functions cooperatively with the OTX/OTD transcription factor CEH-36 to specify an AWC "ground state," and functions with the LIM homeodomain factor LIM-4 to suppress this ground state and drive an AWB identity instead. Our findings provide novel insights into combinatorial codes that drive terminal differentiation programs in the nervous system and reveal a biological function of the deeply conserved Sox2 protein that goes beyond its well-known role in stem cell biology.

Keywords *C. elegans*; neuron differentiation; sox-2; homeodomain
Subject Categories Development & Differentiation; Transcription
DOI 10.15252/embj.201592188 | Received 1 June 2015 | Revised 5 August 2015 | Accepted 6 August 2015 | Published online 4 September 2015
The EMBO Journal (2015) 34: 2574–2589

Introduction

The nervous system is composed of an immense variety of neuronal cell types to process information and control behaviors. This is especially important in developing sensory systems, which generate a large number of specialized neurons for sensing various stimuli in the environment. The molecular mechanisms that control neuronal cell type diversification within sensory systems are only partly understood, and there appear to be substantial differences between cell type diversification within distinct sensory systems and across different animal species (Rister *et al*, 2013).

The *Caenorhabditis elegans* amphids, a pair of bilaterally symmetric sensory organs on the left and right sides of the head, contain twelve neuron pairs whose functions have been defined by laser ablation: Eleven neuron pairs are chemosensory and at least one neuron pair is thermosensory (Bargmann, 2006). These sensory neurons can be distinguished by their cell body morphologies and positions, axonal trajectories, cilia morphologies, synaptic targets, gene expression patterns, and functions (Lanjuin & Sengupta, 2004). Each sensory neuron type expresses characteristic sensory receptor genes and signaling molecules that serve as molecular markers for its cell identity (Bargmann, 2006). Three pairs of olfactory neurons, AWA, AWB, and AWC, are dedicated to sensing volatile odorants. AWA and AWC neurons mediate attraction behaviors toward specific odors, while AWB neurons mediate repulsion away from particular odors (Bargmann, 2006). Unlike other systems in which each olfactory neuron expresses as few as one olfactory G protein-coupled receptor (GPCR) per neuron, worm olfactory neurons coexpress multiple olfactory receptors, possibly more than 20 per cell (Troemel, 1999).

How does the nematode olfactory system develop? AWA, AWB, and AWC share no common lineage history, and their identity is controlled through distinct regulatory programs employing neuron-type-specific terminal selector transcription factors (Lanjuin & Sengupta, 2004; Hobert, 2010). AWA neurons require the *odr-7* nuclear hormone receptor gene for their correct differentiation (Sengupta *et al*, 1994), AWB neurons are specified by the LIM homeobox gene *lim-4* (Sagasti *et al*, 1999), and AWC neurons are specified by the Otx-type homeobox gene *ceh-36* (Lanjuin *et al*, 2003; Kim *et al*, 2010). Each of these selector genes initiates and likely maintains the expression of multiple identity features of the respective olfactory neuron, including olfactory receptors.

1 Department of Biological Sciences, University of Illinois at Chicago, Chicago, IL, USA
2 Molecular and Developmental Biology Graduate Program, University of Cincinnati, Cincinnati, OH, USA
3 Department of Biological Sciences, Department of Biochemistry and Molecular Biophysics, Howard Hughes Medical Institute, Columbia University, New York, NY, USA
*Corresponding author. Tel: +1 312 9964579; E-mail: chioufen.chuang@gmail.com
**Corresponding author. Tel: +1 212 3050063; E-mail: or38@columbia.edu
†These authors contributed equally to this work
‡These authors contributed equally to this work

Intriguingly, loss-of-function mutations in *lim-4* lead to a cell identity transformation, such that AWB identity is lost and an AWC identity is adopted instead (Sagasti *et al*, 1999). Moreover, ectopic expression of *lim-4* in AWC is sufficient to transform AWC to AWB neurons. These results suggest that *lim-4* acts as a molecular switch to distinguish between AWC and AWB neuron identities (Sagasti *et al*, 1999). The molecular basis for this switch behavior lies in the cross-regulation of selector genes. In addition to activating the expression of AWB terminal identity genes (such as the putative odorant receptor *str-1*), *lim-4* also acts in AWB to repress the expression of *ceh-36*, the selector gene of the AWC identity (Kim *et al*, 2010). Lhx7, the murine homolog of *lim-4*, plays a similar role in switching alternative neuron identities, as a deletion of this gene causes a subtype of cholinergic interneurons to convert into another subtype of GABAergic interneurons (Lopes *et al*, 2012).

One key issue that remained unaddressed in previous studies is the problem of specificity. Both the AWB selector gene *lim-4* and the AWC selector gene *ceh-36* are expressed in a number of non-olfactory neuron types (Sagasti *et al*, 1999; Lanjuin *et al*, 2003). By what mechanism is their activity directed toward driving either AWB or AWC identity? We show here that both selector transcription factors operate in the context of a neuron-type-specific combinatorial code that uniquely defines AWB and AWC identities. We find that LIM-4 and CEH-36 each act cooperatively with the HMG-box transcription factor SOX-2 to directly activate terminal differentiation genes to diversify olfactory neuron types. The function of vertebrate Sox2 protein is currently under intense study in the context of stem cell biology. Together with another recent report (Vidal *et al*, 2015), our paper significantly broadens the perspective of Sox2 function by showing that Sox2 can also have a role in terminal neuronal differentiation, through direct regulation of target genes that define the differentiated state of a neuron.

Results

The AWB olfactory neuron is transformed into the AWC^{ON} olfactory neuron in *ky707* mutants

The AWC olfactory neuron pair is morphologically symmetric, but differentiates in late embryogenesis into two asymmetric subtypes, AWC^{ON}, which expresses the GPCR gene *str-2*, and AWC^{OFF}, which expresses the GPCR gene *srsx-3* (Troemel *et al*, 1999; Chuang & Bargmann, 2005; Bauer Huang *et al*, 2007). In wild-type animals, only one of the two AWC neurons becomes the induced AWC^{ON} subtype (Fig 1Ai and B) (Troemel *et al*, 1999). The *ky707* allele was identified from a forward genetic screen for mutants with ectopic expression of the AWC^{ON} cell marker *str-2* in either a single or a pair of non-AWC neurons (Fig 1Aii, Aiii, and B). *ky707* behaved in a recessive manner. The position and morphology of the ectopic AWC^{ON} neurons in *ky707* mutants were similar to those of AWB olfactory neurons. We found that the AWB neurons in *ky707* mutants ectopically expressed a number of additional AWC identity markers, including the GPCR gene *srt-28*, another AWC^{ON} marker (Lesch & Bargmann, 2010), the *ceh-36* Otx-homeobox gene, a key AWC identity selector (Lanjuin *et al*, 2003), and the *eat-4/VGLUT* gene, a defining feature of glutamatergic identity which is normally expressed in AWC, but not AWB neurons (Figs 1B and EV1) (Serrano-Saiz *et al*, 2013). Furthermore, the guanylyl cyclase gene *odr-1*, which is normally expressed in both AWC and AWB neurons (L'Etoile & Bargmann, 2000), but with different expressivity (Lanjuin *et al*, 2003), was expressed in the AWB neurons of *ky707* mutants in a manner characteristic of normal AWC expression (Fig EV1). The *srsx-3* gene, a GPCR-encoding gene asymmetrically expressed in the AWC^{OFF} neuron and the pair of AWB neurons, was lost in AWB in *ky707* mutants (Fig 1B), suggesting that the AWC^{ON} but not AWC^{OFF} identity was adopted by AWB. The *ky707* mutation did not affect the expression of identity markers of 17 other sensory neurons and interneurons examined (Fig EV1).

The adoption of the AWC^{ON} identity by the AWB neurons in *ky707* mutants was paralleled by the loss of the AWB identity. Three AWB identity markers, the *str-1* and *sru-38* GPCR genes and the *lim-4* LIM homeobox gene, failed to be expressed in *ky707* mutants (Figs 1A and B, and EV1). The apparent identity transformation of AWB to AWC in *ky707* mutants is very similar to the transformation observed in animals that lack the *lim-4* LIM homeobox gene (Figs 1B and EV1) (Sagasti *et al*, 1999), suggesting that *lim-4* and the gene responsible for the *ky707* mutant phenotype may work together to distinguish between AWB and AWC neuronal cell identities.

ky707 is a missense mutation in the HMG-box transcription factor gene *sox-2*

ky707 was mapped to a small interval on the X chromosome, and whole-genome sequencing identified a guanine to adenine transition in the *sox-2* gene that results in a glycine (G) to glutamic acid (E) change at the 73rd amino acid of the protein (Fig 2A). The AWB-to-AWC transformation phenotype in *ky707* mutants was rescued with the transgenes, *sox-2p::sox-2* and *sox-2ps::sox-2*, expressing wild-type *sox-2* genomic fragments (Fig 2B and C). In contrast, the transgene *sox-2p::sox-2*^{G73E}, expressing the *ky707* mutant form of *sox-2* genomic fragment, barely rescued the mutant phenotype (Fig 2C). Together, these results support that *ky707* is a missense mutation of *sox-2*.

sox-2 encodes a transcription factor that contains a highly conserved HMG domain at the N-terminus and a diverse serine-rich region at its C-terminus (Fig 2A). The HMG domain is a 79-amino acid protein motif that was shown to interact with DNA and/or other proteins (Lefebvre *et al*, 2007). The C-terminal serine-rich region and the extreme C-terminus of vertebrate Sox2 are essential for transactivation (Ambrosetti *et al*, 2000). There are five predicted *sox* genes in *C. elegans*, eight in *Drosophila melanogaster*, and 20 in mice and humans (Guth & Wegner, 2008). *Caenorhabditis elegans* SOX-2 is a SoxB1-type Sox gene with three vertebrate homologs, Sox1, Sox2, and Sox3. The HMG domain of *C. elegans* SOX-2 protein shares 92% identity to that of human and mouse Sox2 (Figs 2A and EV2). The glycine residue affected by the *ky707* mutation is conserved in the HMG domain of all SoxB1 proteins (Sox1, Sox2, Sox3) as well as in Sry and Sox14 (Fig EV2). However, *C. elegans* SOX-2 and vertebrate SoxB1 proteins do not exhibit any significant homology outside the HMG domain. To determine which of the three vertebrate SoxB1 genes is most functionally conserved with *C. elegans sox-2*, we tested whether mouse Sox1, Sox2, and Sox3 under the control of the *C. elegans sox-2* promoter are able to rescue

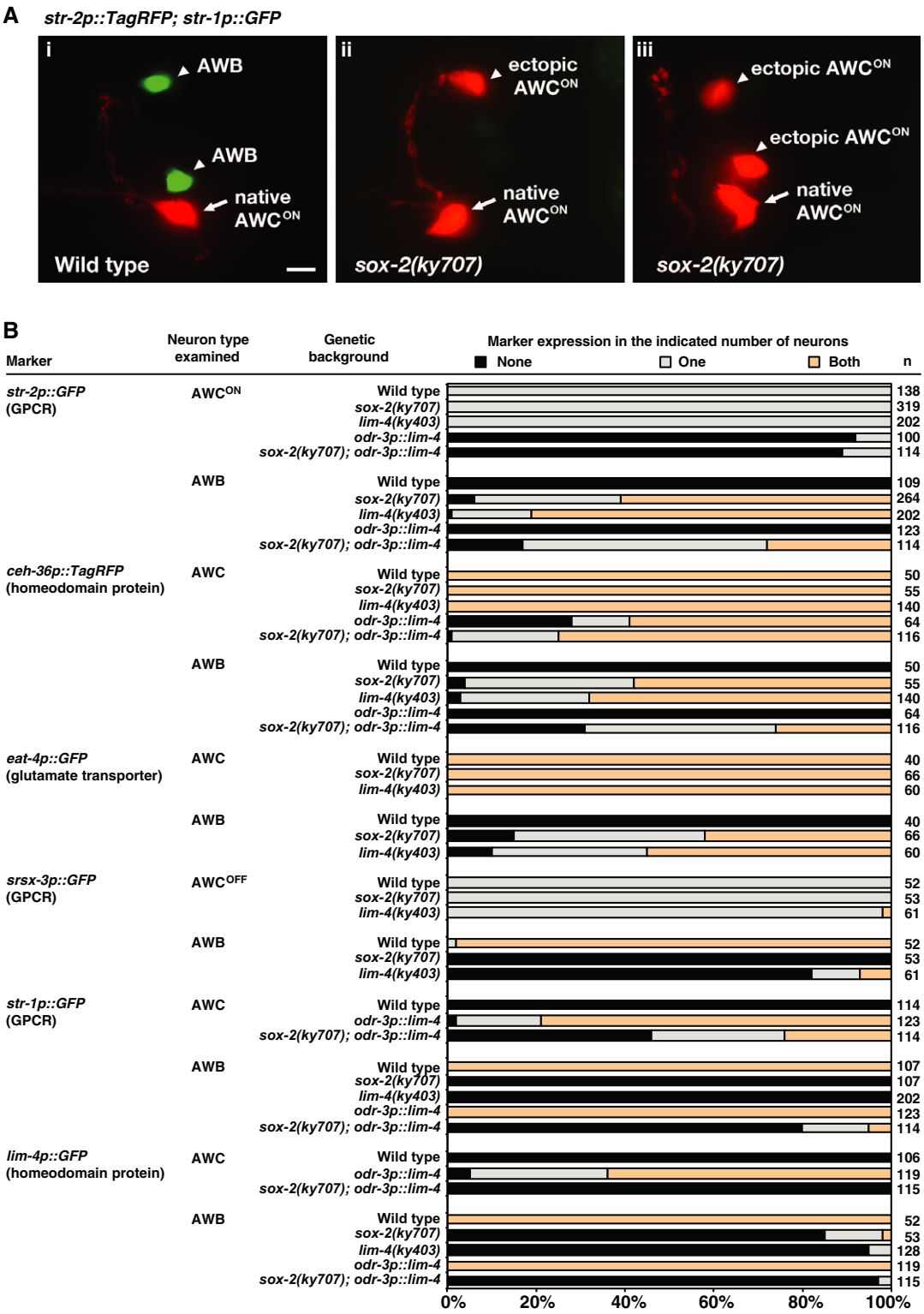

Figure 1. *ky707* mutants lose the expression of AWB identity markers and ectopically express AWC identity markers.

A (Ai) Wild-type animals express *str-2p::TagRFP* in one AWC neuron and *str-1p::GFP* in two AWB neurons. (Aii, Aiii) *ky707* mutants lose expression of *str-1p::GFP* in both AWB neurons and gain expression of *str-2p::TagRFP* in a single AWB neuron (Aii) or in both AWB neurons (Aiii). Anterior is left and ventral is down in ventrolateral views. Scale bar, 5 μm.

B Expression of AWC and AWB markers in *ky707* mutants, *lim-4* mutants, and *odr-3p::lim-4* animals. Animals were scored as adults. *n*, total number of animals scored. GPCR, G protein-coupled receptor. Expression of additional AWC and AWB markers as well as other neuronal markers in *ky707* and *lim-4* mutants is included in Figure EV1.

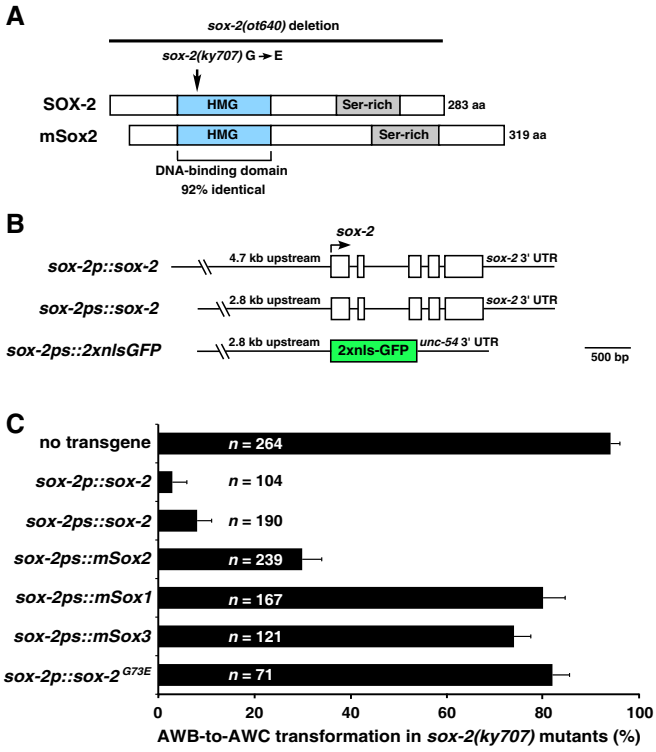

Figure 2. *ky707* is an allele of the HMG-box transcription factor gene *sox-2*.

A Domain structure of *Caenorhabditis elegans* SOX-2 and mouse Sox2 proteins.

B Structure of *sox-2* transgenes.

C Rescue analysis of the AWB-to-AWC transformation phenotype with different *sox-2* and mouse SoxB1 transgenes in *sox-2(ky707)* mutants. AWB-to-AWC transformation was determined by the percentage of animals ectopically expressing the AWC^{ON} marker *str-2p::GFP* in one or two AWB neurons. Error bars indicate standard error of proportion.

sox-2(ky707) mutants. Although the transgenes *sox-2ps::mSox1* and *sox-2ps::mSox3* showed limited rescue of the *ky707* mutant phenotype, *sox-2ps::mSox2* displayed the most efficient rescue (Fig 2C). This suggests functional conservation between *C. elegans* SOX-2 and vertebrate Sox2 proteins.

Cell identity transformation of AWB into AWC^{ON} is partially dependent on the AWC cell identity determination pathway

The specification of native AWC^{ON} identity is regulated by three developmental events, including the specification of general AWC identity, asymmetric differentiation of the two AWC subtypes (one induced AWC^{ON} and one default AWC^{OFF}), and the maintenance of the AWC^{ON} subtype (Fig 3A and Bi) (Lanjuin *et al*, 2003; Kim *et al*, 2010; Taylor *et al*, 2010; Hsieh *et al*, 2014). To determine whether the transformation of AWB to AWC^{ON} in *sox-2(ky707)* mutants is dependent on the genes required for the specification of native AWC^{ON} identity, we introduced mutations in each of these genes in *sox-2(ky707)* mutants (Fig 3B).

The Otx transcription factor CEH-36 is a selector of terminal AWC identity, directly controlling the expression of AWC identity features; the HMX/NKX homeodomain protein MLS-2 is a transiently expressed inducer of *ceh-36* (Fig 3A) (Lanjuin *et al*, 2003; Kim *et al*, 2010). The *sox-2(ky707)* AWB-to-AWC^{ON} transformation phenotype was completely suppressed in *ceh-36(lf)* mutants, but not affected by *mls-2*, demonstrating that *sox-2* cooperates with *ceh-36* but normal *mls-2* input is not required to turn on *ceh-36* expression (Fig 3Bii). Mutations in the AWC^{ON} maintenance genes *nsy-7* (homeodomain-like transcription factor) and *odr-1* (guanylyl cyclase) significantly reduced the *sox-2(ky707)* mutant phenotype (Fig 3Bii) (Troemel *et al*, 1999; Lesch *et al*, 2009). However, the *sox-2(ky707)* mutant phenotype was not significantly changed by mutations in any of the AWC^{ON}/AWC^{OFF} decision genes (Fig 3Bii) (Taylor *et al*, 2010; Hsieh *et al*, 2014). Together, these results suggest that transformation of AWB to AWC^{ON} in *sox-2(ky707)* mutants depends on the AWC identity specification genes and the AWC^{ON} maintenance genes, but is independent of any of the genes required for AWC asymmetry. These results also indicate that native and ectopic AWC^{ON} cells use overlapping but distinct mechanisms to specify and maintain their identities.

The *sox-2(ky707)* mutation causes functional transformation of AWB to AWC^{ON} neurons

AWC^{ON} and AWB olfactory neurons have distinct sensory functions: AWC^{ON} neurons mediate attraction behaviors toward the odor butanone (Wes & Bargmann, 2001), while AWB neurons mediate repulsion behaviors from the odor 2-nonanone (Troemel *et al*, 1997). To determine whether AWB is transformed to AWC^{ON} at functional levels in *sox-2(ky707)* mutants, we performed behavioral assays with AWB- and AWC-sensed odors (Fig 4).

In the avoidance assays with 2-nonanone, wild-type worms were severely repulsed by the odor (Fig 4A and C). In contrast, *sox-2(ky707)* mutants lost their ability to avoid the repulsive odor (Fig 4B and C), suggesting that *ky707* mutants lose AWB neuronal function. In the chemotaxis assays, *sox-2(ky707)* mutants detected the AWC^{ON}-sensed odor butanone normally (Fig 4D). However, *sox-2(ky707)* mutants showed a significantly decreased ability in detecting the AWC^{OFF}-sensed odor 2,3-pentanedione (Fig 4D). This result suggests that the *sox-2(ky707)* mutation may suppress the AWC^{OFF} neuronal function, consistent with the suppression of the *nsy-4(lf)*2AWC^{OFF} phenotype (in which both AWC neurons become AWC^{OFF}) by *sox-2(ky707)* (Fig 3Bi). *nsy-5(ky634)* mutants, which fail to induce AWC^{ON} cells, lost the ability to detect butanone, but chemotaxed normally to 2,3-pentanedione (Fig 4D) (Chuang *et al*, 2007). *nsy-5(ky634); sox-2(ky707)* double mutants, which lose native AWC^{ON} but acquire ectopic AWC^{ON} (Fig 3Bi and Bii), were capable of sensing butanone (Fig 4D). This indicates that the ectopic AWC^{ON} in *sox-2(ky707)* mutants can function as native AWC^{ON} cells. Together, these results suggest a functional transformation of AWB to AWC^{ON} neurons in *sox-2(ky707)* mutants.

To determine whether ectopic AWC neurons adopted native AWC morphology in *sox-2(ky707)* mutants, we analyzed cell body, axon, and cilia morphologies of these neurons in wild-type and *sox-2(ky707)* mutants. The cell body of ectopic AWC neurons in *sox-2(ky707)* mutants had the same round shape as AWB neurons, different from the characteristic oval shape of native AWC cells (Fig EV3A). In addition, the majority of the cilia of ectopic AWC cells displayed variable morphologies more similar to those of

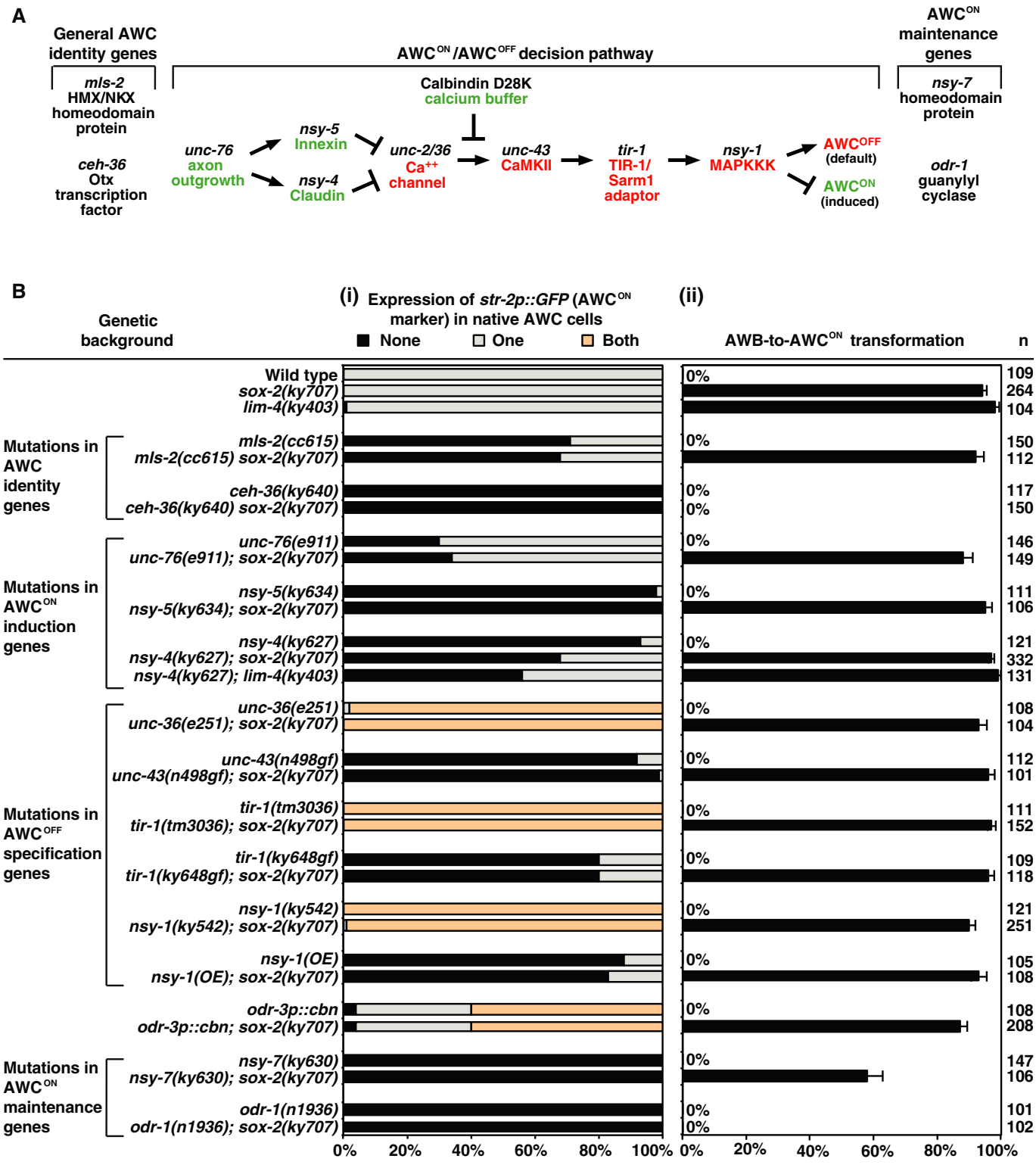

Figure 3. Ectopic expression of the AWC^{ON} marker *str-2::GFP* in *ky707* mutants is partially dependent on the AWC^{ON}/AWC^{OFF} choice pathway.

A The AWC identity determination pathway.

B Expression of the AWC^{ON} marker *str-2p::GFP* in AWC (i) and AWB (ii) neurons in the mutants that are defective in the specification of native AWC identities (Troemel *et al*, 1999; Sagasti *et al*, 2001; Tanaka-Hino *et al*, 2002; Lanjuin *et al*, 2003; Chuang & Bargmann, 2005; Vanhoven *et al*, 2006; Bauer Huang *et al*, 2007; Chuang *et al*, 2007; Lesch *et al*, 2009; Kim *et al*, 2010; Lesch & Bargmann, 2010; Chang *et al*, 2011; Schumacher *et al*, 2012). *n*, total number of animals scored. cbn, calbindin D28K. AWB-to-AWC^{ON} transformation was determined by the percentage of animals ectopically expressing the AWC^{ON} marker *str-2p::GFP* in one or two AWB neurons. Error bars represent standard error of proportion.

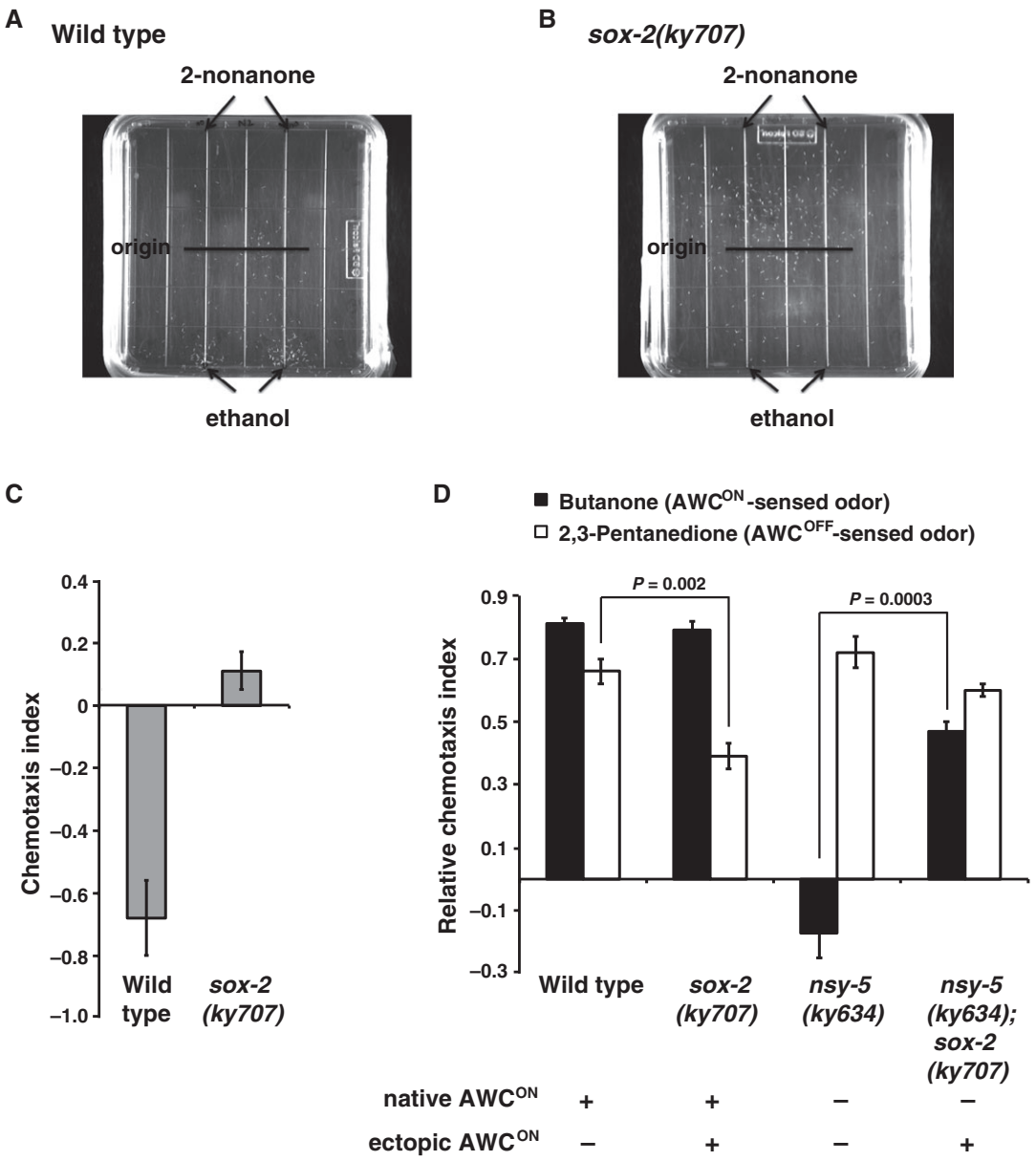

Figure 4. *sox-2(ky707)* mutants lose AWB neuron function and gain ectopic AWC^{ON} sensory function.

A Chemotaxis assay plate of wild-type worms repulsed by the AWB-sensed odor 2-nonanone. White dots on assay plates are individual worms; black lines on plates represent the location where worms were originally placed on the assay plates.

B *sox-2(ky707)* mutants lose repulsion to 2-nonanone.

C Quantification of the level of avoidance to 2-nonanone. A more negative number indicates a more repulsive response. Error bars represent standard error of the mean.

D Quantification of chemotaxis indices of worms to butanone and 2,3-pentanedione. A higher index indicates a higher level of attraction. Error bars represent standard error of the mean. Unpaired Student's *t*-test was used to determine *P*-value.

wild-type AWB cells than native AWC cells (Fig EV3B). These results suggest that the AWB cell body and cilia were not transformed to AWC at the morphological level in *sox-2(ky707)* mutants. However, 45% of ectopic AWC neurons in *sox-2(ky707)* mutants had the S-shaped axon morphology similar to that of native AWC neurons (Fig EV3C). This result suggests that functional transformation of AWB to AWC neurons in *sox-2(ky707)* mutants is mainly correlated with the morphological change in axons. This result is also consistent with the important role of AWB and AWC axons in connecting with different sets of sensory neurons and interneurons for mediating distinct behaviors (White *et al*, 1986).

sox-2 is required to specify both AWB and AWC identities

To further dissect the function of *sox-2* in AWB and AWC cell identity specification, we examined animals carrying a deletion allele of

sox-2, ot640, that eliminates the entire *sox-2* coding region (Vidal *et al*, 2015) and is therefore a null allele. We examined terminal identity markers of AWB and AWC neurons in the *sox-2(ot640)* null mutants, including AWC-specific genes (*str-2, eat-4,* and *ceh-36*), AWB-specific genes (*str-1, lim-4,* and *sru-38*), and genes that are expressed in both AWB and AWC neurons (*odr-1, odr-3, srsx-3*) (Figs 5 and EV4). Unlike *sox-2(ky707)* mutants in which only AWB differentiation was defective, *sox-2(ot640)* null mutants showed severe terminal differentiation defects of both AWB and AWC neurons (Figs 5 and EV4). The only neuron-type-specific identity marker that we found to be unaffected was *odr-3* (Fig EV4). The expression of the pan-neuronal marker *rab-3*, a Ras GTPase gene, and the pan-sensory reporter *ift-20,* an intraflagellar transport gene, was also not affected in AWC and AWB neurons in *sox-2(ot640)* null mutants (Fig EV4). Moreover, the differentiation of the ADF and SAAV neurons (lineal sisters of AWB and AWC, respectively) was not affected in the *sox-2* null mutants (Fig EV4). These observations indicate that *sox-2* controls the terminal differentiation of AWB and AWC, but not their overall generation as neurons, nor does it control earlier lineage decisions. Such differentiation defects are common features of terminal selector transcription factors (Hobert, 2011).

sox-2 acts cell autonomously in AWC and AWB neurons

To examine the site of *sox-2* gene action, we first examined a *sox-2* reporter gene. Since 2.8 kb of sequence upstream of the *sox-2* start codon, combined with the *sox-2* coding sequence, was able to rescue the *sox-2* mutant phenotype (Fig 2B and C), we fused these 2.8 kb of sequences to 2xnls-GFP. This fusion gene was expressed in the nucleus of both AWC and AWB neurons, identified by an integrated *odr-1p::TagRFP* transgene (expressed in AWC and AWB) (Figs 2B and 6A–C). The expression pattern of *sox-2* is consistent with an essential role of *sox-2* in the differentiation of AWC and AWB neurons. The expression of *sox-2* in AWC and AWB is maintained throughout life. *sox-2* is also continuously expressed in other sensory neurons (IL1, IL2, URA, URB, OLL), interneurons (AIM, AIN, AVK, RIH), and motor neurons (RME), as well as in other tissues such as head hypodermis, arcade cells, and rectal epithelial cells (Vidal *et al*, 2015).

To corroborate the notion of cell-autonomous *sox-2* gene function, we performed cell-specific rescue experiments and genetic mosaic analysis. When *sox-2* was expressed in AWB and AWC neurons with the *odr-3* promoter, which is active in the AWB and AWC neurons after they are born (Roayaie *et al*, 1998), the

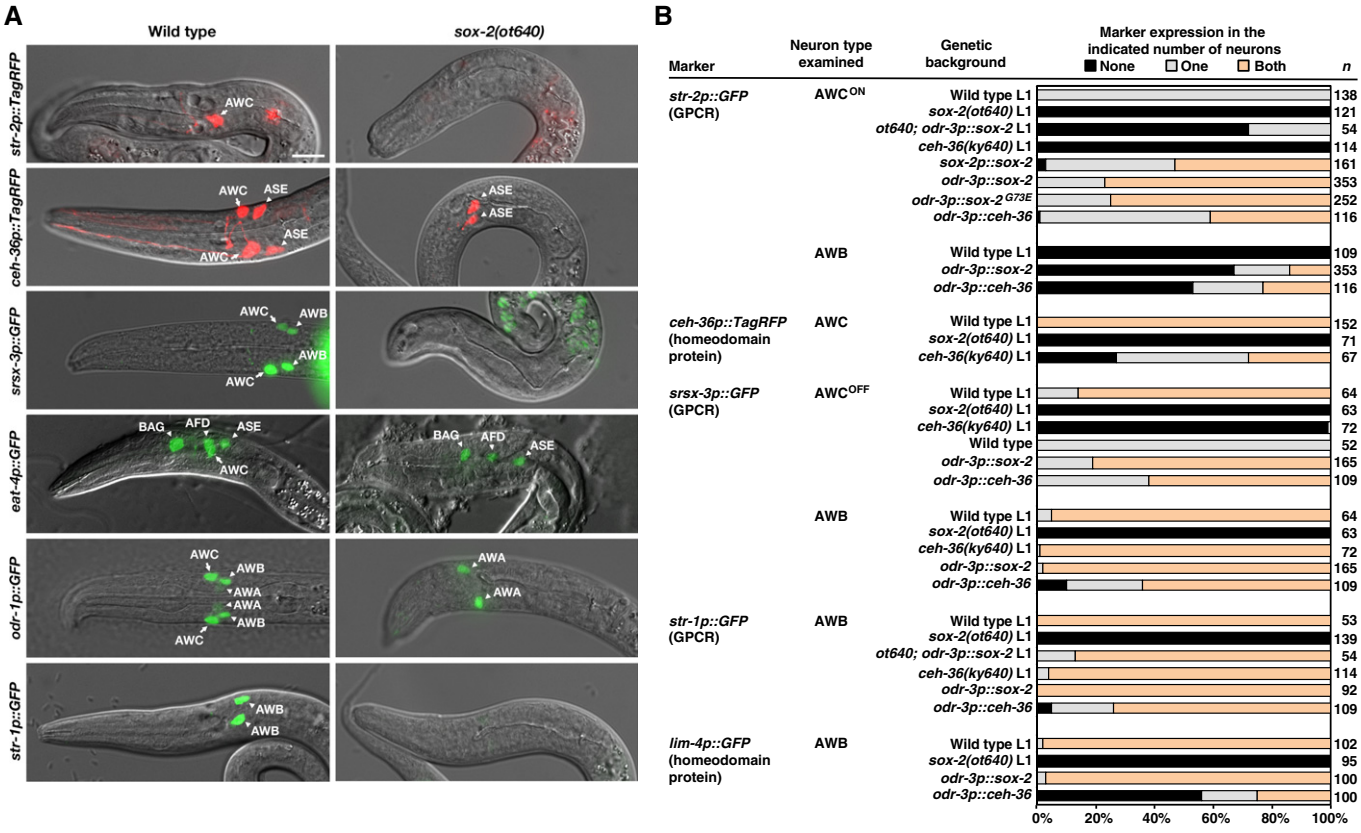

Figure 5. *sox-2* is required for terminal identities of AWC and AWB neurons and may act together with *ceh-36* to specify AWC identities.

A Overlay images of DIC and different AWC and AWB markers in wild-type and *sox-2(ot640)* null mutants. Images were taken at the first larval stage. All *sox-2(ot640)* animals scored displayed the Pun (Pharynx Unattached) phenotype. Anterior is left and ventral is down. Scale bar, 10 μm.

B Expression of selective AWC and AWB markers in *sox-2(ot640)*, *ceh-36(ky640)*, *odr-3p::sox-2*, and *odr-3p::ceh-36* animals. Animals were scored in the first larval stage (L1) or adults. *n*, total number of animals scored. Expression of additional AWC and AWB markers as well as ADF and SAAV neuronal markers in *sox-2(ot640)* and *ceh-36(ky640)* mutants is included in Figure EV4.

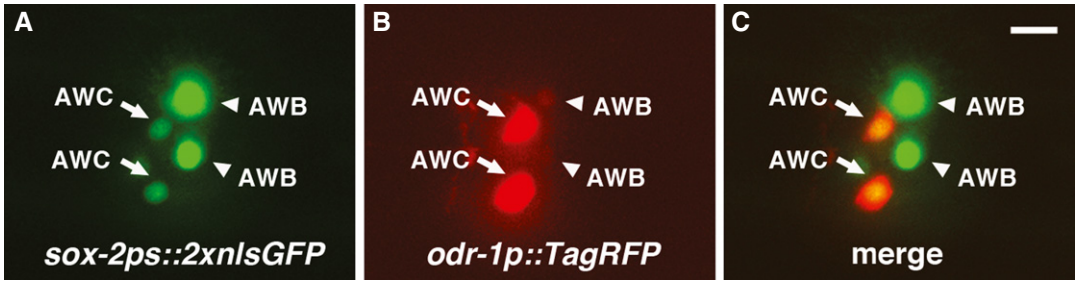

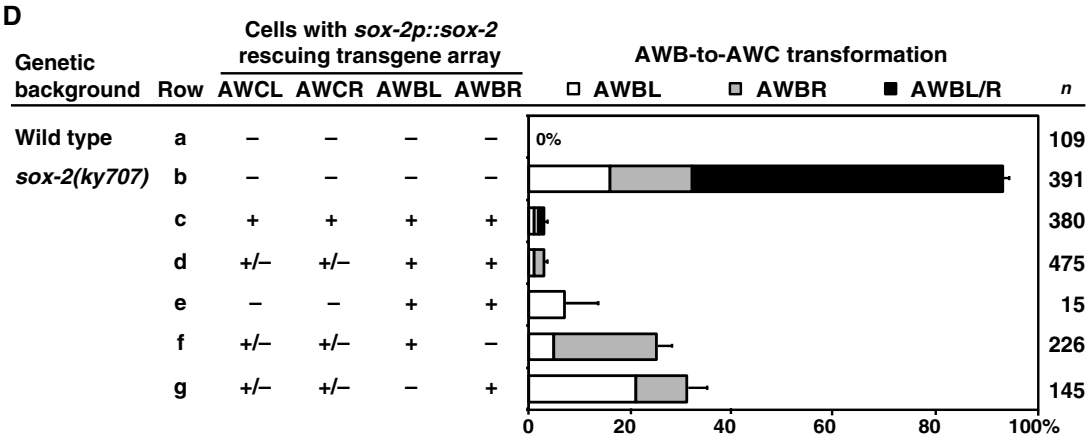

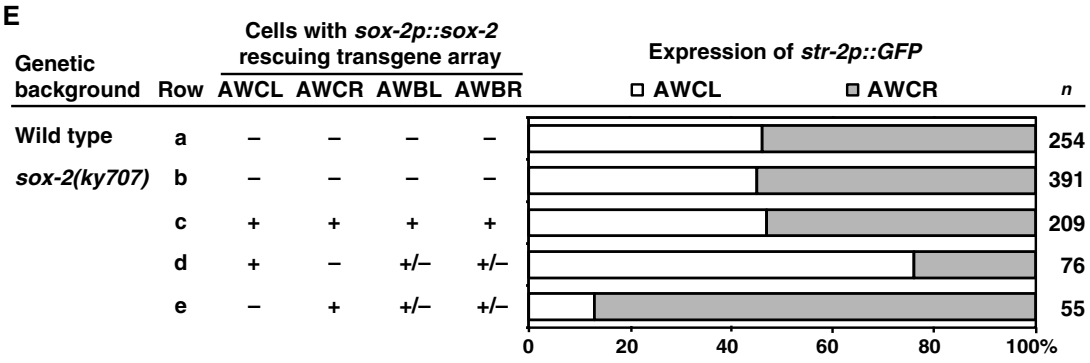

Figure 6. *sox-2* acts cell autonomously in AWC and AWB neurons to regulate their terminal differentiation.

A–C Expression of *sox-2ps::2xnlsGFP* (A) and *odr-1p::TagRFP* (B) in a first-stage larva. Colocalization of GFP and TagRFP in two AWC neurons and two AWB neurons (C). Anterior is left and ventral is down. Scale bar, 5 μm.

D, E Genetic mosaic analysis of animals expressing the rescuing *sox-2p::sox-2; odr-1p::DsRed* transgene in *ky707* mutants. +, cells that retain the transgene array; –, cells that lost the array. *n*, number of mosaic animals scored. Error bars indicate standard error of proportion.

odr-3p::sox-2 transgene almost completely restored the expression of *str-1* in AWB neurons and partially rescued the loss of *str-2* expression in AWC neurons in *sox-2(ot640)* null mutants (Fig 5B).

For the mosaic analysis, we utilized animals expressing the transgene *sox-2p::sox-2* that rescued the *sox-2(ky707)* mutant phenotype (Fig 6D and E). *Caenorhabditis elegans* transgenes are maintained as unstable extrachromosomal arrays, which are spontaneously and randomly lost during mitosis. Mosaic animals were identified by expression of the coinjection marker *odr-1p::DsRed* (expressed in AWC and AWB) that showed which cells retained or lost the rescuing *sox-2p::sox-2* transgene. In non-mosaic animals, the *sox-2p::sox-2* transgene nearly completely rescued the AWB-to-AWC transformation phenotype (Fig 6D, rows a–c). Similar to non-mosaic animals, the majority of mosaic animals that retained the *sox-2p::sox-2* transgene in both AWB cells, regardless of the presence of the transgene in both AWCs, showed efficient rescue of the *sox-2(ky707)* mutant phenotype (Fig 6D, rows d and e). When the *sox-2p::sox-2* transgene was retained in only one of the two

AWB cells, only AWB left (AWBL) or AWB right (AWBR) was transformed to AWC, independent of expression of the transgene in AWC cells (Fig 6D, rows f and g). In more than 74% of these mosaic animals that had one AWB transformed to AWC, the *sox-2p::sox-2*-containing AWB neuron was rescued and the *sox-2(ky707)* mutant AWB was transformed to AWC (Fig 6D, rows f and g). Together, these results are consistent with a cell-autonomous requirement for *sox-2* in differentiating AWB from AWC identities.

We also examined the effect of the *sox-2p::sox-2* transgene on the AWC^{ON}/AWC^{OFF} decision using mosaic analysis (Fig 6E). Similar to wild-type, *sox-2(ky707)* mutants or *sox-2p::sox-2* non-mosaic animals did not show a side bias of AWC^{ON} induction (Fig 6E, rows a–c). When the transgene was retained in only one of the two AWC cells, the *sox-2p::sox-2*-containing AWC neuron became AWC^{ON} and the *sox-2(ky707)* AWC neuron became AWC^{OFF} over 81% of the time (Fig 6E, rows d and e), suggesting that *sox-2* has a cell-autonomous ability to promote AWC^{ON}.

SOX-2 functions cooperatively with CEH-36 and LIM-4 to diversify olfactory neuron types

As described above, the AWB differentiation defects of *sox-2 (ky707)* mutants displayed striking similarities to the AWB differentiation defects of animals that lack the *lim-4* LIM homeobox gene (Figs 1B and EV1). Similarly, the differentiation defects of the AWC neurons in *sox-2* null mutants phenocopied the defects of loss of the *ceh-36* Otx-type homeobox gene in terminally differentiating AWC identity: The expression of *eat-4, str-2*, *srsx-3*, and *odr-1* was lost in AWC neurons in *ceh-36* mutants (Figs 5B and EV4) (Lanjuin *et al*, 2003; Serrano-Saiz *et al*, 2013), as in *sox-2(ot640)* null mutants (Figs 5 and EV4). Taken together, our phenotypic and genetic analysis led us to hypothesize that *sox-2* and *ceh-36* may act together to specify the AWC cell identity and that *sox-2* may function together with *lim-4* to differentiate AWB from AWC identity. In addition, the glycine (G) to glutamic acid (E) substitution at the 73rd residue of the SOX-2 HMG domain in *ky707* mutants may specifically affect the ability of SOX-2 to cooperate with LIM-4, but not CEH-36 (Fig 1B). Protein–protein interactions involving the HMG domain have been previously described (Lefebvre *et al*, 2007; Stros *et al*, 2007).

Mammalian Sox2 has been shown to cooperate with different partner proteins in a variety of cell specification processes (Kamachi & Kondoh, 2013). To directly survey the interactions of SOX-2 with CEH-36 and LIM-4, we expressed wild-type SOX-2, mutant SOX-2^{G73E}, CEH-36, and LIM-4 transcription factors in different combinations in COS-7 cells. The promoter of the AWB/AWC marker *odr-1* (1,027 bp) was used to express the reporter gene luciferase. When transfected alone, each transcription factor had low activity in activating the *odr-1* promoter (Fig 7A). In the cotransfection experiments, we found that CEH-36 and LIM-4 had a cooperative effect on the ability of SOX-2 to activate the *odr-1* promoter (Fig 7A). CEH-36 had a similar cooperative effect with SOX-2 and with SOX-2^{G73E}. However, the cooperative effect of LIM-4 on SOX-2^{G73E} was significantly reduced compared with the effect on SOX-2 (Fig 7A). Since SOX-2^{G73E} cooperated normally with CEH-36, the impaired cooperation with LIM-4 rules out that the SOX-2^{G73E} is less stable or less expressed. These results are consistent with a model in which wild-type SOX-2 functions cooperatively with both CEH-36 and LIM-4, while SOX-2^{G73E} can still function cooperatively with CEH-36 but not with LIM-4 (Fig 8B). This observation provides a mechanistic basis for the observation that the *ky707* allele only affected AWB, but not AWC differentiation. Apart from demonstrating the cooperativity of SOX-2, LIM-4, and CEH-36, the transfection results also demonstrate that these factors operate directly on terminal effectors.

There are several examples of interacting transcription factors that function by cooperative binding to adjacent target sites (Kazemian *et al*, 2013). Therefore, we searched the *odr-1* promoter for putative CEH-36 and LIM-4 binding sites adjacent to SOX-2 consensus sites [SOX-2 sites (Salmon-Divon *et al*, 2010; Engelen *et al*, 2011; Fang *et al*, 2011), LIM-4 sites (Oda-Ishii *et al*, 2005; Flandin *et al*, 2011), CEH-36 sites (Kim *et al*, 2010)]. We identified both predicted LIM-4/SOX-2 and CEH-36/SOX-2 adjacent sites, 2 and 5 base pairs apart, respectively (Fig 7B). The LIM-4/SOX-2 and CEH-36/SOX-2 sites are conserved between *C. elegans* and closely related species *C. remanei*, *C. briggsae*, and *C. brenneri* (Fig 7C and E), suggesting that these sites are potentially important *cis*-regulatory elements. Our promoter-dissecting experiments using GFP reporter transgenes showed that a 393-bp *odr-1* promoter region retaining both LIM-4/SOX-2 and CEH-36/SOX-2 sites was sufficient to drive GFP expression, at the same levels as the reporter driven by a 1,027-bp *odr-1* promoter, in both AWB and AWC neurons (Figs 7B and EV5). In addition, deleting the LIM-4/SOX-2 adjacent sites or mutating either LIM-4 or SOX-2 site in the LIM-4/SOX-2 element in the 393-bp *odr-1* promoter region eliminated the expression of reporter transgenes in AWB without affecting the expression in AWC (Figs 7B and EV5). This suggests that the LIM-4/SOX-2 sites are necessary for *odr-1* expression in AWB. Furthermore, mutating the CEH-36 or SOX-2 binding site in the CEH-36/SOX-2 element caused complete loss or severe reduction of *odr-1* expression in AWC, respectively

Figure 7. The *sox-2(ky707)* mutation reduces LIM-4/SOX-2^{G73E} cooperation but does not affect CEH-36/SOX-2^{G73E} cooperation.

A Quantification of fold activation of *odr-1* promoter measured using dual-spectral luciferase assays in COS-7 cells. The 1,027-bp *odr-1* promoter, expressed in both AWB and AWC neurons, has basal activity in the presence of the single transcription factors CEH-36, LIM-4, SOX-2, or SOX-2^{G73E}. The activity is boosted significantly in the presence of both CEH-36/SOX-2 and LIM-4/SOX-2 combinations. The *sox-2(ky707)* mutation disrupts the cooperation between LIM-4 and SOX-2^{G73E}, but does not affect CEH-36/SOX-2^{G73E} cooperation. All transfection assays were performed in triplicate and repeated three times; three repeats showed similar trends of results. Data of one set of triplicate are presented. Unpaired Student's *t*-test was used to determine *P*-value; ns, not significant.

B *odr-1* promoter GFP reporter constructs and their expression levels in AWB and AWC cells. Increased number of (+) indicates higher intensity of GFP expression; (–) indicates lack of expression. Consensus binding sites of CEH-36, SOX-2, and LIM-4 are boxed. Green, CEH-36 site; blue, SOX-2 site; red, LIM-4 site. Lighter shades of green, blue, and red as well as X represent mutated sites.

C–F EMSA assays of 6×His-tagged proteins with an IRDye-labeled DNA probe containing LIM-4/SOX-2 adjacent binding sites (CSwt) (C, D) or CEH-36/SOX-2 adjacent binding sites (LSwt) (E, F). Nucleotides in gray, light green, light blue, and light red are sequences of *C. remani*, *C. briggsae*, and *C. brenneri* that differ from *C. elegans* sequence. = indicates no alignment available between different species. Sequence alignment between species was performed on http://genome.ucsc.edu. Gel images in (D) and (F) were spliced between lanes 2–3 and 4–5 to exclude irrelevant lanes.

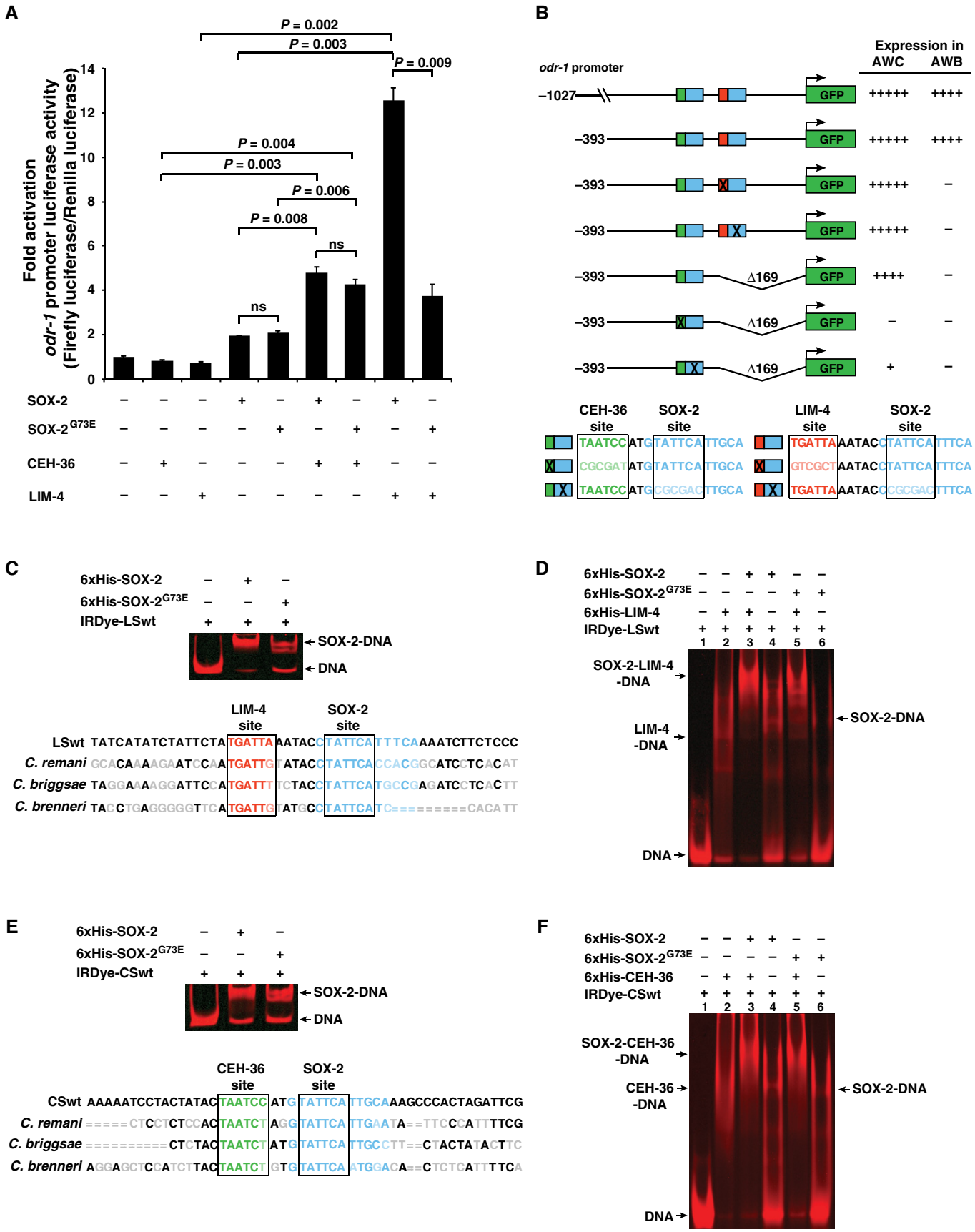

Figure 7.

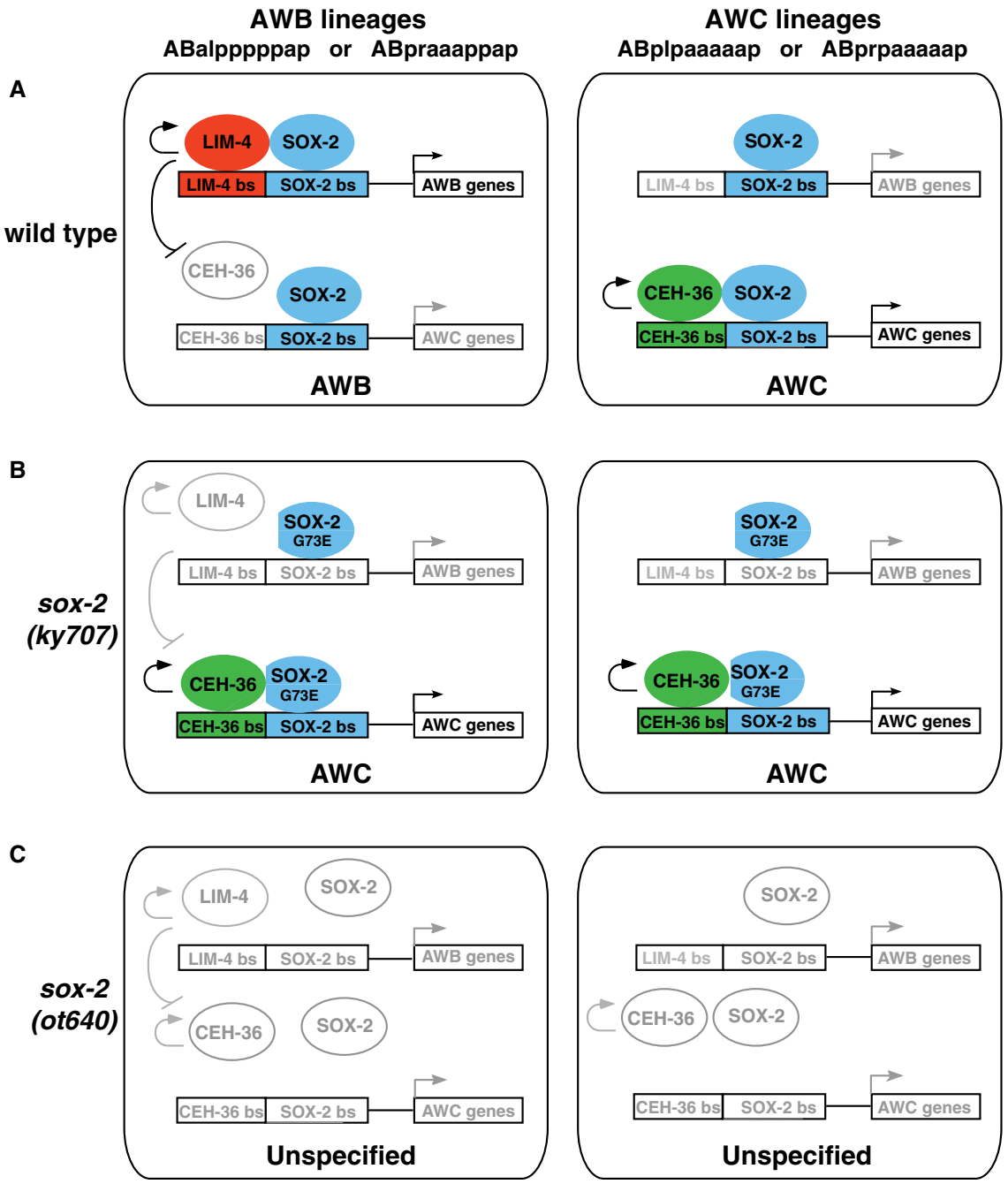

Figure 8. Model of *sox-2* function in alternative differentiation of neuronal subtypes.

A In wild-type, CEH-36 and SOX-2 cooperate to promote AWC identity in AWC precursor cells (right). In AWB precursor cells, SOX-2 cooperates preferentially with LIM-4 to promote AWB identity, thereby preventing CEH-36/SOX-2 to autoregulate and induce AWC identity (left).

B The *sox-2(ky707)* mutation has no effect on the binding of SOX-2^{G73E} to the SOX-2 site in the CEH-36/SOX-2 element, allowing CEH-36/SOX-2^{G73E} cooperation to specify AWC identity in AWC precursor cells (right). The *sox-2(ky707)* mutation specifically reduces the binding of SOX-2^{G73E} to the SOX-2 site in the LIM-4/SOX-2 element, resulting in decreased LIM-4/SOX-2^{G73E} cooperation and consequently enabling CEH-36/SOX-2^{G73E} cooperation to drive AWC identity in AWB precursor cells (left).

C The *sox-2* null allele removes all aspects of *sox-2* activity, resulting in the loss of *lim-4* and *ceh-36* activity and, consequently, AWB and AWC identities.

Autoregulation of *sox-2*, as well as cross-regulation between *sox-2*, *ceh-36*, and *lim-4*, is not represented in the model.

(Figs 7 and EV5). This indicates that the CEH-36/SOX-2 adjacent sites are essential for expression of *odr-1* in AWC. Together, our results are consistent with our genetic data and also support our model that the predicted LIM-4/SOX-2 and CEH-36/SOX-2 sites are essential for *odr-1* expression in AWB and AWC, respectively (Fig 8).

To corroborate that these transcription factors directly bind to their respective predicted target sites, we performed electrophoretic mobility shift assays (EMSAs) using 6×His-tagged proteins and IRDye-labeled probes containing either the CEH-36/SOX-2 or LIM-4/SOX-2 adjacent sites (Appendix Fig S1). Our results show specific binding of SOX-2 to both the CEH-36/SOX-2 and LIM-4/SOX-2 probes, as wild-type unlabeled probes were more efficient at competing with labeled probes in forming the protein–DNA complex than unlabeled probes with mutated SOX-2 binding sites (Appendix Fig S1A and B). CEH-36 and LIM-4 also showed specific binding to the CEH-36/SOX-2 and LIM-4/SOX-2 probes, respectively, since wild-type unlabeled probes were better competitors than the unlabeled probes with a mutated CEH-36 or LIM-4 site (Appendix Fig S1C and D). Both SOX-2 and SOX-2^{G73E} caused a similar degree of shift of the CEH-36/SOX-2 probe (Fig 7E), indicating that the SOX-2^{G73E} mutation does not affect DNA binding to the SOX-2 site in the CEH-36/SOX-2 element. However, SOX-2^{G73E} showed a much reduced level, compared with wild-type SOX-2, in binding to the LIM-4/SOX-2 probe (Fig 7C). To determine the ability of SOX-2 and SOX-2^{G73E} to form a complex with LIM-4 or CEH-36 together with DNA, supershift assays were performed. SOX-2 was more efficient at forming a complex with the LIM-4/SOX-2 probe and LIM-4 protein (Fig 7D, lane 3) than SOX-2^{G73E} (Fig 7D, lane 5). However, SOX-2 and SOX-2^{G73E} had similar levels of ability in forming a complex with CEH-36 and the CEH-36/SOX-2 probe (Fig 7F, lanes 3, 5). Together, these results further suggest a model in which SOX-2 functions cooperatively with both CEH-36 and LIM-4 in a DNA-dependent manner, while SOX-2^{G73E} can still cooperate with CEH-36 through binding to the CEH-36/SOX-2 element but not with LIM-4 due to its reduced binding ability to the LIM-4/SOX-2 element (Fig 8).

Lastly, we note that the *sox-2(ky707)* allele appears to selectively affect the function of *sox-2* in AWB specification (via interaction with LIM-4) since *sox-2(ky707)* mutant animals do not display any of the additional pleiotropies associated with complete loss of *sox-2* function which we recently described [larval lethality, specification of OLL and IL1 sensory neurons (Vidal *et al*, 2015)].

Maintained expression of *sox-2*, *lim-4*, and *ceh-36* depends on auto- and cross-regulation

sox-2, *lim-4*, and *ceh-36* are continuously expressed from embryonic to adult stages, which is consistent with the role of these transcription factors in the initiation of a terminal differentiation program and the maintenance of the differentiated state. It was previously shown that *lim-4* autoregulates its expression in AWB and *ceh-36* autoregulates in AWC (Appendix Fig S2) (Sagasti *et al*, 1999; Kim *et al*, 2010). To determine (i) whether *sox-2* also autoregulates, and (ii) whether these transcription factors also cross-regulate, we examined the expression of each factor in *sox-2(null)*, *sox-2(ky707)*, *ceh-36(lf)*, and *lim-4(lf)* mutants (Appendix Fig S2).

The expression of the *sox-2ps::2xnlsGFP* reporter gene was significantly reduced in AWC neurons in *sox-2(ot640)* null mutants as well as in AWB neurons in *sox-2(ot640)* and *sox-2(ky707)* mutants (Appendix Fig S2), suggesting that *sox -2* regulates its own expression in both AWC and AWB. In addition, the expression of *sox-2ps::2xnlsGFP* was significantly reduced in AWC in *ceh-36 (ky640lf)* mutants and in AWB in *lim-4(ky403lf)* mutants (Appendix Fig S2), suggesting that *ceh-36* and *lim-4* are required for *sox-2* expression in AWC and AWB, respectively. Furthermore, the expression of a *ceh-36p::GFP* reporter gene in AWC and a *lim-4p::GFP* reporter gene in AWB was significantly reduced in *sox-2(ot640)* null mutants (Appendix Fig S2), suggesting that *sox-2* regulates *ceh-36* and *lim-4* expression in AWC and AWB, respectively. Together, these results suggest that maintained expression of *sox-2*, *lim-4*, and *ceh-36* is achieved through autoregulation and cross-regulation.

Gene dosage experiments suggest a competition model

The data presented so far demonstrate two main features of AWB and AWC differentiation (schematically summarized in Fig 8): (i) SOX-2 and LIM-4 cooperate in AWB to induce AWB identity and to prevent the adoption of the alternative AWC identity by repressing the expression of the *ceh-36* gene, an inducer of AWC identity, and (ii) CEH-36 cooperates with SOX-2 to induce AWC identity in AWC neurons of wild-type animals or in AWB in *lim-4* or *sox-2(ky707)* mutants (in which the cooperation of SOX-2 with LIM-4 is affected). Since *sox-2* is required for both the AWB and AWC differentiation programs, we considered a competition model. In this model, LIM-4 may repress the alternative AWC identity in AWB by preferentially cooperating with SOX-2, thereby limiting the access of CEH-36 to SOX-2. Since SOX-2 and CEH-36 are required for *ceh-36* expression itself, the ultimate output of LIM-4's preferential cooperation with SOX-2 is a failure to express *ceh-36* and hence AWC identity. Although we are unable to observe *ceh-36* expression in AWB neurons in wild-type animals, it may be transiently expressed in embryonic AWB neurons and suppressed fairly quickly by *lim-4*.

We tested the competition model by probing specific predictions of the model. First, this model would predict that ectopic expression of *lim-4* in the AWC neurons is sufficient to induce AWB identity in AWC and to repress *ceh-36* expression and hence AWC identity. We found that ectopic *lim-4* expression in AWC from the *odr-3p::lim-4* transgene indeed repressed *ceh-36* expression in AWC (Fig 1B), resulting in loss of terminal AWC identity (Fig 1B) (Sagasti *et al*, 1999). In addition, ectopic *lim-4* expression in AWC induced the expression of AWB markers *str-1* and *lim-4* (Fig 1B), as previously reported (Sagasti *et al*, 1999). Moreover, the ectopic induction of AWB identity by ectopic *lim-4* expression in AWC genetically required the presence of wild-type *sox-2* (Fig 1B).

Vice versa, the competition model predicts that overexpression of *ceh-36* in AWB from the *odr-3p::ceh-36* transgene may be able to promote CEH-36/SOX-2 cooperation in AWB and thereby overcome the normally preferred LIM-4/SOX-2 cooperation, resulting in the induction of AWC identity in AWB and loss of AWB identity. We found this to be indeed the case: The AWC marker *str-2* was induced and the AWB markers *str-1* and *lim-4* were reduced (Fig 5B).

Lastly, the competition model predicts that SOX-2 is present in rate-limiting amounts in AWB, so that all available SOX-2 cooperates only with LIM-4. Raising the level of SOX-2 in AWB should make SOX-2 become available for cooperation with CEH-36. This should result in the induction of AWC identity in AWB, but in this case, normal AWB identity should be unaffected because LIM-4 can still cooperate with SOX-2 to also induce AWB identity. We indeed observed a mixed AWB/AWC identity of AWB neurons in animals

that expressed *sox-2* under control of the *odr-3* promoter from the *odr-3p::sox-2* transgene: The AWC marker *str-2* was induced and the AWB markers *str-1* and *lim-4* were unaffected (Fig 5B). This also suggests that overexpression of *sox-2* may be able to bypass *lim-4* repression of *ceh-36* in AWB neurons.

Taken together, even though we cannot rule out alternative scenarios, our data suggest that SOX-2 can partner with both LIM-4 and CEH-36, but preferential partnering of LIM-4 with SOX-2 is able to overcome a CEH-36/SOX-2-driven "AWC ground state" that would normally be executed in AWC and AWB in the absence of *lim-4*.

Distinct differentiation mechanisms for distinct olfactory neuron types

One key aspect of the *sox-2*-dependent AWB/AWC differentiation event is the concept of a *ceh-36/sox-2*-dependent "AWC ground state" that is modified by *lim-4* to drive AWB and inhibit AWC identity in a *sox-2* dependent manner. Several previous studies have suggested that AWC is also a default identity state for several other amphid sensory neuron classes, as this ground state is revealed upon removal of the terminal selector gene of the respective amphid sensory identity. Specifically, loss of AWA identity in *odr-7* or *lin-11* mutants, loss of ASG identity in *unc-130; odr-7* double mutants, or loss of AFD identity in *ttx-1* mutants has been proposed to reveal an AWC ground state (Sagasti *et al*, 1999; Sarafi-Reinach & Sengupta, 2000; Sarafi-Reinach *et al*, 2001; Satterlee *et al*, 2001; Lanjuin *et al*, 2003). However, these conclusions were mainly if not exclusively based on the ectopic expression of the GPCR *str-2*, an AWC^{ON} marker. *str-2* has been found to be exquisitely sensitive to various sensory signals and sensory activity (Peckol *et al*, 2001; Nolan *et al*, 2002), and the change in *str-2* expression may therefore not necessarily reflect a cell identity switch. We revisited this issue by examining whether another AWC^{ON} marker *srt-28* (GPCR gene), the AWC terminal identity marker *odr-1* (guanylyl cyclase gene), and the AWC terminal selector *ceh-36* (Otx-homeobox gene) are indeed derepressed if the identity of other amphid sensory neurons is lost, as would be expected from the AWC default model. We found that only the *srt-28* marker, like *str-2*, was ectopically expressed in AWA in *odr-7* mutants, but no evidence of identity switches from other amphid sensory neurons to AWC in *odr-7, lin-11,* or *ttx-1* mutants when *odr-1* and *ceh-36* markers were examined (Appendix Fig S3). These results collectively suggest that AWC is not the default state of AWA, ASG, or AFD neurons. Taken together with previous studies, our findings indicate that olfactory sensory neurons are specified in fundamentally distinct manners. AWB and AWC share a common ground state, even though these neurons are lineally unrelated, but other olfactory (AWA), gustatory (ASG), or thermosensory (AFD) neurons do not develop from this common "ground state,"

Discussion

We have identified a novel role of *sox-2* in postmitotic specification and differentiation of two distinct, but related types of sensory neurons, the olfactory AWB and AWC neuron types, in *C. elegans*. Previous work has demonstrated a role of *sox-2* in controlling the terminal differentiation of postmitotic neuron types (Vidal *et al*, 2015), yet the mechanistic basis for how *sox-2* fulfills such function has been unclear. We define here a competition mechanism by which two distinct homeodomain factors can compete for cooperation with *sox-2* to drive neuron-type-specific gene expression programs.

Several studies have shown that cooperative interactions of vertebrate Sox2 with various partner factors determine target gene specificity, thereby providing a code of cell specification (Kamachi & Kondoh, 2013). For example, Sox2 interaction with Brn2 defines a neural progenitor state (Lodato *et al*, 2013), the Sox2-Pax6 partnership specifies lens development (Kamachi *et al*, 2001), Sox2 and Gli cooperate in Shh-directed neural tube patterning (Peterson *et al*, 2012), and Sox2 functions with Tcf/Lef to repress cyclin D1 (Hagey & Muhr, 2014). Our results suggest a model in which SOX-2 cooperates with either LIM-4 or CEH-36 to distinguish between the AWB versus the AWC olfactory neuron identity (Fig 8). In AWC neurons, SOX-2 cooperates with CEH-36 as a terminal selector to activate transcription of AWC-specific genes through binding to the CEH-36/SOX-2 adjacent sites (Fig 8A). In AWB neurons, SOX-2 pairs with LIM-4 to act as a terminal selector for AWB identity by binding to the LIM-4/SOX-2 adjacent sites (Fig 8A). The pairing of LIM-4 and CEH-36 with SOX-2 generates unique combinatorial transcription factor codes that define the specificity of action of LIM-4 and CEH-36, each of which is expressed in additional, different neuron types that do not express SOX-2.

In addition, *lim-4* represses *ceh-36* expression and therefore prevents the execution of the alternative AWC identity in AWB (Fig 8A). This repression may be direct or it may be the result of a competition of LIM-4 with CEH-36 for cooperation with SOX-2, with LIM-4 being the preferred SOX-2 partner, thereby preventing SOX-2/CEH-36-mediated AWC induction. Gene dosage experiments that we performed favor the competition model.

The *sox-2(ky707)* mutation causes a glycine to glutamic acid change in the highly conserved HMG-box domain. The HMG-box domain of Sox proteins has multiple important roles in the regulation of target gene expression through binding to DNA and/or interacting with different partner proteins (Lefebvre *et al*, 2007). The AWB-to-AWC transformation phenotype resulting from the *sox-2(ky707)* mutation suggests that the mutation may change the binding specificity of SOX-2 with the target genes and/or its interacting proteins in AWB neurons. Our electrophoretic mobility shift assay results suggest the mutant $SOX\text{-}2^{G73E}$ can still cooperate with CEH-36 through binding to the CEH-36/SOX-2 element, while $SOX\text{-}2^{G73E}$ is no longer able to cooperate with LIM-4 due to its reduced binding ability to the LIM-4/SOX-2 element. This leads to the derepression of the SOX-2/CEH-36 partnership in AWB cells, causing them to transform into AWC neurons (Fig 8B). When SOX-2 is abolished, as in *sox-2(ot640)* null mutants, both AWB and AWC identities are lost (Fig 8C). Taken together, CEH-36 and SOX-2 define an "AWC ground state" on which the AWB identity is superimposed by LIM-4 cooperating with SOX-2, which induces AWB identity and represses AWC identity. "AWC identity" is the ground state only for the AWB and AWC neurons, and it is not a general ground state for other olfactory and sensory neurons as previously proposed (Sagasti *et al*, 1999; Sarafi-Reinach *et al*, 2001; Lanjuin *et al*, 2003).

The competition mechanism by which AWB and AWC neurons are specified bears striking similarities to the specification of the ALM and BDU neurons that we recently described (Gordon &

Hobert, 2015). In both cases, two neurons share a common terminal selector (SOX-2 in AWB and AWC; UNC-86 in ALM and BDU) that pairs up with a distinct cofactor to distinguish between identities of different neuron types (SOX-2/LIM-4 pair in AWB and SOX-2/CEH-36 pair in AWC; UNC-86/MEC-3 pair in ALM and UNC-86/PAG-3 pair in BDU). Another similarity observed is that one of the cofactors (LIM-4 in AWB and MEC-3 in ALM) outcompetes the other potential cofactor (CEH-36 in AWB and PAG-3 in ALM) for cooperation with the terminal selector. Hence, the loss of either cofactor (LIM-4 in AWB and MEC-3 in ALM) results in what essentially amounts to a homeotic transformation in cellular identity (AWB to AWC as described here; ALM to BDU as described in Gordon and Hobert (2015)). Having observed such a mechanism in two completely different cellular contexts suggests that it may be a common principle that distinct neuron types may share a common terminal selector, which pair up with distinct cofactors in a competitive manner. In an evolutionary context, this principle may mean that neuron identities may diversify from an ancestral ground state through the recruitment of a terminal selector into a new cellular context where it can cooperate with a resident terminal selector to drive a novel cellular identity.

Since a number of SOX and homeobox genes are highly expressed in adult human olfactory bulb (Marei *et al*, 2012) and since the binding motifs of homeodomain proteins and SOX family proteins are overrepresented in the promoters of mouse olfactory receptor genes (Plessy *et al*, 2012), we propose that the role of Sox2 in olfactory neuron specification may be conserved in vertebrates and that Sox2 may operate with as yet to be identified homeodomain proteins to fulfill this function in vertebrates.

Materials and Methods

Strains and transgenes

Wild-type is strain N2, *C. elegans* variety Bristol. Strains were maintained by standard methods (Brenner, 1974). Animal care and use were carried out in accordance with the Institutional Biosafety Committee Policies. A list of strains and transgenes can be found in the Appendix Supplementary Methods. Power analysis was used to determine the sample size that is adequate to detect a significant effect size.

Forward genetic screen

Forward genetic screen was performed as previously described (Brenner, 1974). P0 animals were mutagenized with EMS. Five F1 progenies were then transferred onto single plates, and F2 worms were screened for mutants using the Zeiss fluorescence compound microscope. The *ky707* mutant was identified from a screen of 2,400 genomes.

Genetic mapping and whole-genome sequencing

Three-factor mapping experiments were performed to map *ky707* to chromosome X between *unc-6(n102)* (X:-2.01) and *dpy-7(e88)* (X:-1.65). Whole-genome sequencing of the *ky707* mutant was performed on an Illumina GA2x sequencing platform, using 100-nucleotide reads. Sequencing results were analyzed with the MAQGene software as previously described (Bigelow *et al*, 2009).

Plasmid construction

A list of plasmid DNA can be found in the Appendix Supplementary Methods.

Behavioral assays

Chemotaxis assays were performed and chemotaxis indices were computed as in previous studies (Bargmann *et al*, 1993; Troemel *et al*, 1997). 2-butanone (Sigma 360473) and 2,3-pentanedione (Sigma 241962) were diluted 1:1,000 and 1:10,000, respectively, in ethanol. About 50-150 animals were assayed for each strain and each odor in each individual assay. All assays were performed four independent times.

Mammalian cell transfection and luciferase assays

Mammalian expression constructs were transfected into COS-7 cells using the Lipofectamine 2000 reagent (Invitrogen) in a 24-well format according to the manufacture's protocol. A control vector (gift of J. Wells, Cincinnati Children's) expressing *Renilla* Luciferase from the CMV promoter was used for normalizing transfection efficiency. The total amount of DNA was kept constant with addition of the pcDNA6 V5 6×His A empty vector. Cell lysates were prepared 48 h after transfection, and luciferase activity was measured using the Firefly & *Renilla* Luciferase Assay Kit (Biotium) and GloMax-96 Microplate Luminometer (Promega). All transfection assays were performed in triplicate and repeated three times.

6×His-tagged protein expression and purification

To make 6×His-tagged proteins, *sox-2*, *sox-2*^{G73E}, *lim-4*, and *ceh-36* were cloned into pRSETA (Invitrogen) and transformed into BL21-CodonPlus(DE3)-RIL bacterial cells (Stratagene). IPTG (0.1 or 1 mM) was added in transformed cell culture (OD_{600} = ~0.7) to induce 6×His-tagged protein expression for 1–4 h at 37°C. Cells were then harvested and lysed with B-PER in phosphate buffer (Thermo Scientific Pierce). 6×His-tagged proteins were purified using a HisPur Cobalt Purification Kit (Thermo Scientific Pierce). SDS–PAGE and Coomassie staining were used to determine the purity and concentration of purified 6×His-tagged proteins.

Electrophoretic mobility shift assay (EMSA)

To make IRDye-labeled probes, long oligonucleotides (51–52-mers, IDT) and complementary short oligonucleotides (13–14-mers, IDT) with 5′ IR-700 dye modification were annealed, and 5′ overhangs were filled in with Klenow DNA polymerase (NEB). Long oligonucleotides of complementary sequences were annealed to make unlabeled probes for competition analysis with IRDye-labeled probes. Purified 6×His-tagged proteins (80–200 ng), unlabeled probes (10–125 nM, only added for competition experiments in Appendix Fig S1), and IRDye-labeled probes (5 nM) were incubated at room temperature in 1× binding buffer (10 mM Tris–HCl pH 7.5, 10 mM NaCl, 40 mM KCl, 1 mM $MgCl_2$, 1 mM EDTA pH 8.0, 5%

glycerol, and 50 μg/ml BSA) for 15 min and resolved in a pre-run 5% polyacrylamide gel containing 2.5% glycerol in 0.5× TBE buffer. The small gel (8.3 cm width × 7.3 cm length × 0.75 mm thickness, Bio-Rad Mini-PROTEAN; Fig 7C and E; Appendix Fig S1) was run at 80 V for up to 75 min, and the large gel (16 cm width × 14 cm length × 1.5 mm thickness, Thermo Scientific Owl P9DS dual gel vertical electrophoresis; Fig 7D and F) was run for 3 h. The gel was imaged using a LICOR Odyssey CLx Infrared Imaging System.

Expanded View for this article is available online:
http://emboj.embopress.org

Acknowledgements
This work was supported by a Choose Ohio First Scholarship (A.A.), a National Institutes of Health (NIH) Organogenesis Training Grant (Y.-W.H.), the NSF (IOS-1455758 to C.C.), the March of Dimes Foundation (C.C.), Whitehall Foundation Research Awards (C.C. and C.-F.C), Alfred P. Sloan Research Fellowship (C.-F.C.), the Howard Hughes Medical Institute (O.H.), and the NIH (5R01GM111320-02 to C.C., R01NS039996-05 and R01NS050266-03 to O.H., and 5R01GM098026-05 to C.-F.C.). The *ky707* allele was isolated by C.-F.C. as a postdoctoral fellow in Cori Bargmann's laboratory. We thank Cori Bargmann and Piali Sengupta for neuronal marker strains, Alex Boyanov for whole-genome sequencing of the *ky707* mutant, Maria Doitsidou for assistance in MAQGene analysis of whole-genome sequencing results, Kyle McCracken and Jim Wells for advice on cell transfection and luciferase assays, Brian Gebelein for advice on EMSAs, Yutaka Yoshida for mouse cDNA, Andy Fire for *C. elegans* vectors, and *C. elegans* Genetic Center, which is funded by NIH Office of Research Infrastructure Programs (P40 OD010440), for strains.

Author contributions
AA, Y-WH, BV, CC, OH, and C-FC conceived or designed the experiments. AA, Y-WH, BV, and C-FC performed the experiments. AA, Y-WH, BV, CC, OH, and C-FC analyzed the data. AA, Y-WH, OH, and C-FC wrote the manuscript.

Conflict of interest
The authors declare that they have no conflict of interest.

References

Ambrosetti DC, Scholer HR, Dailey L, Basilico C (2000) Modulation of the activity of multiple transcriptional activation domains by the DNA binding domains mediates the synergistic action of Sox2 and Oct-3 on the fibroblast growth factor-4 enhancer. *J Biol Chem* 275: 23387 – 23397

Bargmann CI, Hartwieg E, Horvitz HR (1993) Odorant-selective genes and neurons mediate olfaction in *C. elegans*. *Cell* 74: 515 – 527

Bargmann CI (2006) Chemosensation in *C. elegans*. WormBook, ed. The *C. elegans* Research Community, WormBook, doi: 10.1895/wormbook.1.123.1.

Bauer Huang SL, Saheki Y, VanHoven MK, Torayama I, Ishihara T, Katsura I, van der Linden A, Sengupta P, Bargmann CI (2007) Left-right olfactory asymmetry results from antagonistic functions of voltage-activated calcium channels and the Raw repeat protein OLRN-1 in *C. elegans*. *Neural Dev* 2: 24

Bigelow H, Doitsidou M, Sarin S, Hobert O (2009) MAQGene: software to facilitate *C. elegans* mutant genome sequence analysis. *Nat Methods* 6: 549

Brenner S (1974) The genetics of *Caenorhabditis elegans*. *Genetics* 77: 71 – 94

Chang C, Hsieh YW, Lesch BJ, Bargmann CI, Chuang CF (2011) Microtubule-based localization of a synaptic calcium-signaling complex is required for left-right neuronal asymmetry in *C. elegans*. *Development* 138: 3509 – 3518

Chuang CF, Bargmann CI (2005) A Toll-interleukin 1 repeat protein at the synapse specifies asymmetric odorant receptor expression via ASK1 MAPKKK signaling. *Genes Dev* 19: 270 – 281

Chuang CF, Vanhoven MK, Fetter RD, Verselis VK, Bargmann CI (2007) An innexin-dependent cell network establishes left-right neuronal asymmetry in *C. elegans*. *Cell* 129: 787 – 799

Engelen E, Akinci U, Bryne JC, Hou J, Gontan C, Moen M, Szumska D, Kockx C, van Ijcken W, Dekkers DH, Demmers J, Rijkers EJ, Bhattacharya S, Philipsen S, Pevny LH, Grosveld FG, Rottier RJ, Lenhard B, Poot RA (2011) Sox2 cooperates with Chd7 to regulate genes that are mutated in human syndromes. *Nat Genet* 43: 607 – 611

Fang X, Yoon JG, Li L, Yu W, Shao J, Hua D, Zheng S, Hood L, Goodlett DR, Foltz G, Lin B (2011) The SOX2 response program in glioblastoma multiforme: an integrated ChIP-seq, expression microarray, and microRNA analysis. *BMC Genom* 12: 11

Flandin P, Zhao Y, Vogt D, Jeong J, Long J, Potter G, Westphal H, Rubenstein JL (2011) Lhx6 and Lhx8 coordinately induce neuronal expression of Shh that controls the generation of interneuron progenitors. *Neuron* 70: 939 – 950

Gordon PM, Hobert O (2015) A Competition Mechanism for a Homeotic Neuron Identity Transformation in *C. elegans*. *Dev Cell* 34: 206 – 219

Guth SI, Wegner M (2008) Having it both ways: Sox protein function between conservation and innovation. *Cell Mol Life Sci* 65: 3000 – 3018

Hagey DW, Muhr J (2014) Sox2 acts in a dose-dependent fashion to regulate proliferation of cortical progenitors. *Cell Rep* 9: 1908 – 1920

Hobert O (2010) Neurogenesis in the nematode *Caenorhabditis elegans*. WormBook, ed. The *C. elegans* Research Community, WormBook, doi: 10.1895/wormbook.1.12.2.

Hobert O (2011) Regulation of terminal differentiation programs in the nervous system. *Annu Rev Cell Dev Biol* 27: 681 – 696

Hsieh YW, Alqadah A, Chuang CF (2014) Asymmetric neural development in the *Caenorhabditis elegans* olfactory system. *Genesis* 52: 544 – 554

Kamachi Y, Uchikawa M, Tanouchi A, Sekido R, Kondoh H (2001) Pax6 and SOX2 form a co-DNA-binding partner complex that regulates initiation of lens development. *Genes Dev* 15: 1272 – 1286

Kamachi Y, Kondoh H (2013) Sox proteins: regulators of cell fate specification and differentiation. *Development* 140: 4129 – 4144

Kazemian M, Pham H, Wolfe SA, Brodsky MH, Sinha S (2013) Widespread evidence of cooperative DNA binding by transcription factors in Drosophila development. *Nucleic Acids Res* 41: 8237 – 8252

Kim K, Kim R, Sengupta P (2010) The HMX/NKX homeodomain protein MLS-2 specifies the identity of the AWC sensory neuron type via regulation of the ceh-36 Otx gene in *C. elegans*. *Development* 137: 963 – 974

Lanjuin A, VanHoven MK, Bargmann CI, Thompson JK, Sengupta P (2003) Otx/otd homeobox genes specify distinct sensory neuron identities in *C. elegans*. *Dev Cell* 5: 621 – 633

Lanjuin A, Sengupta P (2004) Specification of chemosensory neuron subtype identities in *Caenorhabditis elegans*. *Curr Opin Neurobiol* 14: 22 – 30

Lefebvre V, Dumitriu B, Penzo-Mendez A, Han Y, Pallavi B (2007) Control of cell fate and differentiation by Sry-related high-mobility-group box (Sox) transcription factors. *Int J Biochem Cell Biol* 39: 2195 – 2214

Lesch BJ, Gehrke AR, Bulyk ML, Bargmann CI (2009) Transcriptional regulation and stabilization of left-right neuronal identity in *C. elegans*. *Genes Dev* 23: 345 – 358

Lesch BJ, Bargmann CI (2010) The homeodomain protein hmbx-1 maintains asymmetric gene expression in adult *C. elegans* olfactory neurons. *Genes Dev* 24: 1802 – 1815

L'Etoile ND, Bargmann CI (2000) Olfaction and odor discrimination are mediated by the *C. elegans* guanylyl cyclase ODR-1. *Neuron* 25: 575 – 586

Lodato MA, Ng CW, Wamstad JA, Cheng AW, Thai KK, Fraenkel E, Jaenisch R, Boyer LA (2013) SOX2 co-occupies distal enhancer elements with distinct POU factors in ESCs and NPCs to specify cell state. *PLoS Genet* 9: e1003288

Lopes R, Verhey van Wijk N, Neves G, Pachnis V (2012) Transcription factor LIM homeobox 7 (Lhx7) maintains subtype identity of cholinergic interneurons in the mammalian striatum. *Proc Natl Acad Sci USA* 109: 3119 – 3124

Marei HE, Ahmed AE, Michetti F, Pescatori M, Pallini R, Casalbore P, Cenciarelli C, Elhadidy M (2012) Gene expression profile of adult human olfactory bulb and embryonic neural stem cell suggests distinct signaling pathways and epigenetic control. *PLoS One* 7: e33542

Nolan KM, Sarafi-Reinach TR, Horne JG, Saffer AM, Sengupta P (2002) The DAF-7 TGF-beta signaling pathway regulates chemosensory receptor gene expression in *C. elegans*. *Genes Dev* 16: 3061 – 3073

Oda-Ishii I, Bertrand V, Matsuo I, Lemaire P, Saiga H (2005) Making very similar embryos with divergent genomes: conservation of regulatory mechanisms of Otx between the ascidians Halocynthia roretzi and Ciona intestinalis. *Development* 132: 1663 – 1674

Peckol EL, Troemel ER, Bargmann CI (2001) Sensory experience and sensory activity regulate chemosensory receptor gene expression in *Caenorhabditis elegans*. *Proc Natl Acad Sci USA* 98: 11032 – 11038

Peterson KA, Nishi Y, Ma W, Vedenko A, Shokri L, Zhang X, McFarlane M, Baizabal JM, Junker JP, van Oudenaarden A, Mikkelsen T, Bernstein BE, Bailey TL, Bulyk ML, Wong WH, McMahon AP (2012) Neural-specific Sox2 input and differential Gli-binding affinity provide context and positional information in Shh-directed neural patterning. *Genes Dev* 26: 2802 – 2816

Plessy C, Pascarella G, Bertin N, Akalin A, Carrieri C, Vassalli A, Lazarevic D, Severin J, Vlachouli C, Simone R, Faulkner GJ, Kawai J, Daub CO, Zucchelli S, Hayashizaki Y, Mombaerts P, Lenhard B, Gustincich S, Carninci P (2012) Promoter architecture of mouse olfactory receptor genes. *Genome Res* 22: 486 – 497

Rister J, Desplan C, Vasiliauskas D (2013) Establishing and maintaining gene expression patterns: insights from sensory receptor patterning. *Development* 140: 493 – 503

Roayaie K, Crump JG, Sagasti A, Bargmann CI (1998) The G alpha protein ODR-3 mediates olfactory and nociceptive function and controls cilium morphogenesis in *C. elegans* olfactory neurons. *Neuron* 20: 55 – 67

Sagasti A, Hobert O, Troemel ER, Ruvkun G, Bargmann CI (1999) Alternative olfactory neuron fates are specified by the LIM homeobox gene lim-4. *Genes Dev* 13: 1794 – 1806

Sagasti A, Hisamoto N, Hyodo J, Tanaka-Hino M, Matsumoto K, Bargmann CI (2001) The CaMKII UNC-43 activates the MAPKKK NSY-1 to execute a lateral signaling decision required for asymmetric olfactory neuron fates. *Cell* 105: 221 – 232

Salmon-Divon M, Dvinge H, Tammoja K, Bertone P (2010) PeakAnalyzer: genome-wide annotation of chromatin binding and modification loci. *BMC Bioinformatics* 11: 415

Sarafi-Reinach TR, Sengupta P (2000) The forkhead domain gene unc-130 generates chemosensory neuron diversity in *C. elegans*. *Genes Dev* 14: 2472 – 2485

Sarafi-Reinach TR, Melkman T, Hobert O, Sengupta P (2001) The lin-11 LIM homeobox gene specifies olfactory and chemosensory neuron fates in *C. elegans*. *Development* 128: 3269 – 3281

Satterlee JS, Sasakura H, Kuhara A, Berkeley M, Mori I, Sengupta P (2001) Specification of thermosensory neuron fate in *C. elegans* requires ttx-1, a homolog of otd/Otx. *Neuron* 31: 943 – 956

Schumacher JA, Hsieh YW, Chen S, Pirri JK, Alkema MJ, Li WH, Chang C, Chuang CF (2012) Intercellular calcium signaling in a gap junction-coupled cell network establishes asymmetric neuronal fates in *C. elegans*. *Development* 139: 4191 – 4201

Sengupta P, Colbert HA, Bargmann CI (1994) The *C. elegans* gene odr-7 encodes an olfactory-specific member of the nuclear receptor superfamily. *Cell* 79: 971 – 980

Serrano-Saiz E, Poole RJ, Felton T, Zhang F, De La Cruz ED, Hobert O (2013) Modular Control of Glutamatergic Neuronal Identity in *C. elegans* by Distinct Homeodomain Proteins. *Cell* 155: 659 – 673

Stros M, Launholt D, Grasser KD (2007) The HMG-box: a versatile protein domain occurring in a wide variety of DNA-binding proteins. *Cell Mol Life Sci* 64: 2590 – 2606

Tanaka-Hino M, Sagasti A, Hisamoto N, Kawasaki M, Nakano S, Ninomiya-Tsuji J, Bargmann CI, Matsumoto K (2002) SEK-1 MAPKK mediates Ca2 + signaling to determine neuronal asymmetric development in *Caenorhabditis elegans*. *EMBO Rep* 3: 56 – 62

Taylor RW, Hsieh YW, Gamse JT, Chuang CF (2010) Making a difference together: reciprocal interactions in *C. elegans* and zebrafish asymmetric neural development. *Development* 137: 681 – 691

Troemel ER, Kimmel BE, Bargmann CI (1997) Reprogramming chemotaxis responses: sensory neurons define olfactory preferences in *C. elegans*. *Cell* 91: 161 – 169

Troemel ER (1999) Chemosensory signaling in *C. elegans*. *BioEssays* 21: 1011 – 1020

Troemel ER, Sagasti A, Bargmann CI (1999) Lateral signaling mediated by axon contact and calcium entry regulates asymmetric odorant receptor expression in *C. elegans*. *Cell* 99: 387 – 398

Vanhoven MK, Bauer Huang SL, Albin SD, Bargmann CI (2006) The claudin superfamily protein nsy-4 biases lateral signaling to generate left-right asymmetry in *C. elegans* olfactory neurons. *Neuron* 51: 291 – 302

Vidal B, Santella A, Serrano-Saiz E, Bao Z, Chuang CF, Hobert O (2015) *C. elegans* SoxB genes are dispensable for embryonic neurogenesis but required for terminal differentiation of specific neuron types. *Development* 142: 2464 – 2477

Wes PD, Bargmann CI (2001) *C. elegans* odour discrimination requires asymmetric diversity in olfactory neurons. *Nature* 410: 698 – 701

White JG, Southgate E, Thomson JN, Brenner S (1986) The structure of the nervous system of the nematode *Caenorhabditis elegans*. *Philos Trans R Soc Lond B Biol Sci* 314: 1 – 340